

Improvement of damage-assessment results using high-spatial density measurements

R. Pascual^{a,*}, R. Schälchli^b, M. Razeto^b

^a *Department of Mechanical Engineering, Universidad de Chile, Casilla 2777, Santiago, Chile*

^b *Department of Mechanical Engineering, Universidad de Concepción, Casilla 53-C, Concepción, Chile*

Abstract

Model-based damage assessment is based on measuring the distance between experimental and analytical results. In practice, measurements yield only partial mode shapes with respect to the total degrees of freedom present in the corresponding finite element model. Thus, before any damage detection method is implemented, the experimental mode shape has to be expanded to the same dimension of the numerical mode shape. Mode shapes expansion is a key point in the damage localisation process, since actual defects of the structure may be hidden by expansion errors. This paper introduces a new general procedure to the expansion/damage assessment process using an optimised choice for: the size of the expansion basis, the number of experimental degrees of freedom and the sensor placement. We introduce a new indicator to evaluate the problems inherent to the expansion/damage detection process using the minimisation of error on constitutive equations (MECE) technique. It provides insight of the inherent limitations of MECE and helps the decision making process on how many degrees of freedom should be measured and how many mode shapes should be used in the expansion basis. The procedure is illustrated using a finite element model of a plate-like structure, where the damage state is simulated as a reduction of the local stiffness.

Keywords: Mode shape expansion; High-spatial density measurements; Damage detection; Finite element

1. Introduction

In recent years, a great effort has been put forward to assess damage in structures using vibration measurements. The vibration and model based damage identification methods rely on the fact that the occurrence of damage in a structural system leads to changes in the

*Corresponding author. Tel.: + 56-2-6784591; fax: + 56-2-6896057.

E-mail address: rpascual@ing.uchile.cl (R. Pascual).

Nomenclature

K, M	finite element model stiffness and mass matrices
K* , M*	experimental matrices
ω^*	experimental frequency
Z	dynamic stiffness matrix at ω
$\Delta\mathbf{Z}$	error in the dynamic stiffness matrix
ϕ	i th numerical mode shape
$\Delta\mathbf{f}$	residual force vector related to \mathbf{v}
$\bar{\omega}$	measured frequency for $\bar{\mathbf{v}}$
\mathbf{v}	expanded experimental mode shape
\mathbf{v}^*	experimental vector
$\bar{\mathbf{v}}$	measured mode shape
\mathbf{u}	instrument mode shape associated to \mathbf{v}
\mathbf{K}_s	s th elementary stiffness matrix in global coordinates
$\tilde{\mathbf{K}}$	condensed stiffness matrix
e_s	energy in element s
Θ	equilibrium weight matrix
Ξ	regularisation weight matrix
Φ	model modal matrix
\mathbf{q}	modal displacements
\mathbf{q}^*	perfectly estimated modal coordinates
α	control parameter
n_n	number of numerical modes employed for expansion
n_{fe}	number of degrees of freedom of the FE model
n_e	number of elements of the FE model
n_m	number of measured degrees of freedom
T	expansion operator
μ	modal mass matrix associated to Φ

Superscripts

*	experimental
<i>se</i>	SEREP
<i>me</i>	MECE

Subscripts

<i>m</i>	measured set of degrees of freedom
----------	------------------------------------

Abbreviations

FE	Finite element
SEREP	System equivalent Reduction Expansion Process
MECE	Minimisation of Errors in Constitutive Equations
DOFs	Degrees Of Freedom

dynamic properties of the structure. These changes may be used to assess the state of damage of a structure.

In this article, we introduce a new indicator to investigate the problems inherent to the expansion/damage localisation procedure using the minimisation of errors on constitutive equations (MECE) technique [1]. This indicator allows us to evaluate the limitations that appear when the expanded mode shapes are a combination of a limited set of FE eigenmodes. A considerable restriction in the number of analytical mode shapes in the expansion basis may cause a deficient error localisation, because actual defects of the structure may be hidden by expansion errors.

1.1. State of the art

Several model based structural damage detection methods can be found in the literature. They vary on how and what experimental data is used in the methods. Some researchers used changes in modal parameters to locate structural damage; others prefer the forced responses.

Salawu [2] published a survey on the use of natural frequency changes for damage diagnostics. The shift in the natural frequencies have some practical limitations to damage localisation. The low sensitivity of the natural frequency shifts to damage requires very precise measurements or large levels of damage. The modal frequencies are a global property of the structure and they generally can not provide spatial information about the structural damage.

Ratcliffe [3] used the Laplacian operator on the mode shapes to locate damage. When the damage is severe, the results are successful. However, when the damage is incipient, further processing of the Laplacian output is required. Higher frequency mode shapes were not effective to locate damage since they tend to show only local displacements.

Pandey et al. [4] employed the change in the mode shapes curvature to detect damage. The curvatures are obtained using a central difference approximation. In a situation with little displacements, the curvature approximation becomes very sensitive to the presence of noise. The method seems to work properly with higher frequency mode shapes. However, as the number of modes increases, measurements become more expensive to carry on.

Shi et al. [5] suggested the use of the change of the modal strain energy in each element before and after the occurrence of damage. Unfortunately, elements corresponding to nodal points of the mode shape show exceptionally large and small values of the modal strain energy, and this fact may give a wrong indication of the damage location.

Lee and Shin [6] introduced a frequency-domain method of structural damage identification. This method was formulated from the dynamic stiffness equation of motion. The method does not seem to be suitable for large FE models because the number of unknown damage magnitudes is much more larger than the measured degree of freedom (DOFs). Thus, it is necessary to derive more linear algebraic equations to make the damage identification well posed. In other words, as the finite elements number increases, more measurements are required.

Ren et al. [7] proposed the residual modal force damage index method to predict the damage location and severity. Their formulation starts from the error of equilibrium resulting from substituting the measured modal data into the structure eigenvalue equation. An inconvenience is that the method presents two types of different variables: forces and moments. In order to

compare results, it is necessary to scale these two contributions. Nevertheless, the comparison is not evident.

Messina et al. [8] proposed an assurance criterion to identify the amount of damage at multiple sites. The method is based on the sensitivity of the natural frequency of each mode to damage in each site. If the number of potential damaged sites is large, the computational cost becomes very high. In a multiple damage situation, it is necessary to consider several of the modes shapes whose frequencies change significantly, and for each of them, to identify a list of potentially damaged sites. Any restriction to the set of locations to be searched could end in an inaccurate damage localisation. In the same field, Kim and Stubbs [9] proposed an improved algorithm to locate and estimate severity of damage in structures using changes in modal characteristics. They assumed that all the nodal points are measured; however in practice it is almost impossible to have the same number of experimental and numerical degrees of freedom.

Gawronski and Sawicki [10] proposed a structural damage localisation procedure using modal and sensor norms. Unfortunately, their approach involves knowing a priori the location of the damage, since the structures are more densely meshed near the damage locations so as to better reflect the stress concentration.

Thyagarajan et al. [11] investigated an optimisation procedure to update the FE model matrices to the damage state. The limitation of the technique is that it requires a lot of computing which may restrict it to small models. A large number of design variables would cause a divergence of the optimisation procedure.

In this general scenario we by-pass the difficulties mentioned in the published papers taking advantage of the great amount of information provided by numerical models (FE) and high-spatial density vibration measurements.

2. MECE expansion/error localisation

The dynamic equilibrium equation of the experimental structure corresponding to a particular mode shape \mathbf{v}^* may be written as

$$\mathbf{K}^* \mathbf{v}^* = \omega^{*2} \mathbf{M}^* \mathbf{v}^*, \quad (1)$$

where \mathbf{K}^* and \mathbf{M}^* respect the same connectivity pattern as the finite element matrices \mathbf{K} and \mathbf{M} , respectively. Without any loss of generality, the damping terms are not considered. This development is intended to explain how the method works. The assumption of such a structural model for the experimental structure, considers in an implicit way a linear behaviour. Also, there exists an instrument vector \mathbf{u} that satisfies the equilibrium equation:

$$\mathbf{K} \mathbf{u} = \bar{\omega}^2 \mathbf{M} \mathbf{v}, \quad (2)$$

where \mathbf{K} and \mathbf{M} are numerical quantities, $\bar{\omega}$ is the measured frequency and \mathbf{v} is the experimental expanded vector for $\bar{\omega}$. Note that superscript $*$ refers to actual experimental responses and system matrices. They differ of the measured responses (noise is present) and also of the expanded responses (expansion error appear due to noise and model errors). The correspondence between

the experimental structure and the FE model may be established through the following relations:

$$\begin{aligned}\mathbf{K}^* &= \mathbf{K} + \Delta\mathbf{K}^*, \\ \mathbf{M}^* &= \mathbf{M} + \Delta\mathbf{M}^*\end{aligned}\quad (3)$$

and the assumed experimental mode shape \mathbf{v}^* (and its frequency ω^*) can be broken down into the expanded experimental vector \mathbf{v} plus the errors $\Delta\mathbf{v}$ and $\Delta\omega$:

$$\begin{aligned}\mathbf{v}^* &= \mathbf{v} + \Delta\mathbf{v}, \\ \omega^* &= \bar{\omega} + \Delta\omega\end{aligned}\quad (4)$$

2.1. Expansion of the experimental information

Expansion techniques consider the transformation of the shape vectors exclusively. The expanded vector \mathbf{v} may be sought by minimising the residue of the equilibrium equation in some adequate metric Θ :

$$\min_{\mathbf{v}} \Delta\mathbf{f}^T \Theta \Delta\mathbf{f}, \quad (5)$$

where

$$\Delta\mathbf{f} = (\mathbf{K} - \bar{\omega}^2\mathbf{M})\mathbf{v} = \mathbf{Z}\mathbf{v}, \quad (6)$$

Complementing the objective function (5), the distance between the expanded vector and the experimental vector may be also minimised:

$$\min_{\mathbf{v}} (\mathbf{v}_m - \bar{\mathbf{v}})^T \Xi (\mathbf{v}_m - \bar{\mathbf{v}}), \quad (7)$$

where the subscript m represents the measured set of DOFs. Subtracting Eqs. (2) and (6) we obtain the equation that relates the MECE objective with the general objective (5):

$$\Delta\mathbf{f} = \mathbf{K}(\mathbf{v} - \mathbf{u}). \quad (8)$$

Considering both conditions (5) and (7) in one single hybrid objective function and using Eq. (8) we obtain

$$\min_{\mathbf{v}} (\mathbf{v} - \mathbf{u})^T \mathbf{K}(\mathbf{v} - \mathbf{u}) + \alpha (\mathbf{v}_m - \bar{\mathbf{v}})^T \tilde{\mathbf{K}}(\mathbf{v}_m - \bar{\mathbf{v}}), \quad (9)$$

with the static flexibility matrix for the equilibrium term $\Theta = \mathbf{K}^{-1}$ and the reduced stiffness matrix for the regularisation term $\Xi = \tilde{\mathbf{K}}$. A variation is to express the expanded mode shape as a linear combination of certain number of mode shapes of the model:

$$\mathbf{v} = \Phi\mathbf{q}, \quad (10)$$

where Φ has n_n modes. The system equivalent reduction expansion process (SEREP) expansion [12] represents the experimental vector as a linear combination of certain number of numerical mode shapes. The best estimate for the modal displacements is found by the least squares pseudo-inverse Φ_m^+ :

$$\mathbf{q}^{se} = \Phi_m^+ \bar{\mathbf{v}}. \quad (11)$$

Replacing the reduced stiffness matrix $\Xi = \mathbf{K}^{se}$ defined by the SEREP operator in problem (9), it may be written as

$$\min_{\mathbf{v}} (\mathbf{u} - \mathbf{v})\mathbf{K}(\mathbf{u} - \mathbf{v}) + \alpha(\bar{\mathbf{v}} - \mathbf{v}_m)^T \mathbf{K}^{se}(\bar{\mathbf{v}} - \mathbf{v}_m). \quad (12)$$

Next, problem (12) may be expressed as

$$\min_{\mathbf{q}^{me}} (\mathbf{u} - \mathbf{v})^T \mathbf{K}(\mathbf{u} - \mathbf{v}) + \alpha(\mathbf{v} - \mathbf{v}^{se})^T \mathbf{K}(\mathbf{v} - \mathbf{v}^{se}). \quad (13)$$

If \mathbf{K} and \mathbf{M} are expressed in terms of their modal decomposition [13], we obtain the following expression for the MECE modal displacement in terms of the SEREP modal displacement:

$$\mathbf{q}^{me} = \alpha[(\mathbf{I} - \bar{\omega}^2 \mathbf{\Omega}^{-2})^2 + \alpha \mathbf{I}]^{-1} \mathbf{q}^{se}, \quad (14)$$

where $\mathbf{\Omega}$ is a diagonal matrix containing the numerical eigenfrequencies associated with $\mathbf{\Phi}$.

2.2. Damage assessment

The objective of the error localisation methods is to detect the location where the damage or model errors may be present.

2.2.0. MECE indicator

From problems (5) and (8), it is straightforward to define an element level error indicator closely related to the MECE expansion:

$$e_s = (\mathbf{u} - \mathbf{v})^T \mathbf{K}_s(\mathbf{u} - \mathbf{v}). \quad (15)$$

If several experimental modes are used in the analysis, the contribution of the mode shape \mathbf{v} may be normalised by

$$e_s = \frac{(\mathbf{u} - \mathbf{v})^T \mathbf{K}_s(\mathbf{u} - \mathbf{v})}{(\mathbf{u} - \mathbf{v})^T \mathbf{K}(\mathbf{u} - \mathbf{v})}. \quad (16)$$

2.3. Limitations of the MECE localisation

We observe several sources of problems when using the MECE indicator. They may be inherent to the indicator associated to the experimental mode shape and due to the expansion method.

2.3.1. Excitation of model errors

The residual force can be expressed as a sum of two terms:

$$-\Delta \mathbf{f} = \mathbf{Z}\Delta \mathbf{v} + \Delta \mathbf{Z}^* \mathbf{v}^*, \quad (17)$$

where the first term on the right hand is dependent on the criterion used for the expansion and the second one is an unknown constant. If errors are localised, the non spurious component of the residual force is a sparse vector, almost full of zeros. Non-zero values are dependent on the ability of the experimental mode shape \mathbf{v}^* to excite the substructure(s) that present(s) errors ($\Delta \mathbf{Z}^*$):

$$\Delta \mathbf{f}^* = \Delta \mathbf{Z}^* \mathbf{v}^* \gg 0. \quad (18)$$

A potentially dangerous situation for error localisation is to identify a mode shape which does not excite the error:

$$\Delta \mathbf{Z}^* \mathbf{v}^* \approx 0. \quad (19)$$

Modes verifying Eq. (19) are blind to model errors. It is necessary for the expanded vector to produce a good level of deformation in the substructures where error might be present. This problem is not addressed in this work.

2.3.2. Scattering of the residual energy

Eq. (8) establishes that the residual displacement vector $\mathbf{v} - \mathbf{u}$ is the solution of the equivalent static problem:

$$\mathbf{K}(\mathbf{v} - \mathbf{u}) = \Delta \mathbf{f}. \quad (20)$$

The solution of problem (20) results in residual deformations distributed over the structure. The damaged elements will inevitably affect the dynamic behaviour of the neighbouring elements, because they are sharing at least one DOF. For this reason, the strain energy error indicator (15) will show scattered residual energies.

2.3.3. Limited expansion basis

To describe the limitations of using a set of numerical mode shapes for the expansion we start from Eq. (2):

$$\mathbf{u} = \bar{\omega}^2 \mathbf{K}^{-1} \mathbf{M} \mathbf{v}. \quad (21)$$

If the expanded vector \mathbf{v} is constrained by Eq. (10) and a spectral development of \mathbf{K}^{-1} is used, \mathbf{u} may also be expressed as

$$\mathbf{u} = \bar{\omega}^2 \sum_{j=1}^{n_{fe}} \frac{\phi_j \phi_j^T}{\omega_j^2 \mu_j} \mathbf{M} \left(\sum_{k=1}^{n_n} q_k \phi_k \right), \quad (22)$$

where q_k corresponds to the estimated modal displacement associated to ϕ_k . Eq. (22) can be simplified to

$$\mathbf{u} = \sum_{j=1}^{n_n} \left(\frac{\bar{\omega}}{\omega_j} \right)^2 q_j \phi_j. \quad (23)$$

This results allows us to express the content of the residual vector $\mathbf{v} - \mathbf{u}$, whose strain energy distribution will be used for damage assessment:

$$\mathbf{v} - \mathbf{u} = \sum_{j=1}^{n_n} \left(1 - \left(\frac{\bar{\omega}}{\omega_j} \right)^2 \right) q_j \phi_j. \quad (24)$$

Since $\mathbf{v} - \mathbf{u}$ is built up by combining a limited set of modes shapes, its energy content will be limited to what these modes shapes are able to represent. Eq. (24) may also be written as

$$\mathbf{v} - \mathbf{u} = \mathbf{\Phi} \hat{\mathbf{q}} \quad (25)$$

with

$$\hat{\mathbf{q}} = (\mathbf{I} - \bar{\omega}^2 \mathbf{\Omega}^{-2}) \mathbf{q}. \quad (26)$$

Fortunately, the richness of the experimental information provided by a laser Doppler vibrometer (LDV) allows us to consider a great number of mode shapes in the expansion basis. Considering a large number of mode shapes in the expansion basis, the residual forces are reproduced in a more accurate way, therefore the damage detection will provide more accurate results.

2.4. Deciding the size of the expansion basis

Eq. (25) can be useful to select the number of mode shapes that should be in the expansion basis Φ , since it needs to be wide enough to show peaks of the residual energy at the substructure where parametric error might be present. It would be interesting to establish for each substructure s the maximum of the residual energy it may carry:

$$\Pi_s^m = \max_{\forall \mathbf{v}-\mathbf{u}} \frac{(\mathbf{v} - \mathbf{u})^T \mathbf{K}_s (\mathbf{v} - \mathbf{u})}{(\mathbf{v} - \mathbf{u})^T \mathbf{K} (\mathbf{v} - \mathbf{u})} \quad (27)$$

under constraint (25). The problem may be rewritten as

$$\Pi_s^m = \max_{\forall \mathbf{v}-\mathbf{u}} \frac{\hat{\mathbf{q}}^T (\Phi^T \mathbf{K}_s \Phi) \hat{\mathbf{q}}}{\hat{\mathbf{q}}^T (\Phi^T \mathbf{K} \Phi) \hat{\mathbf{q}}} \quad (28)$$

which is written as the standard Rayleigh quotient [14]:

$$\Pi_s^m = \max_{\forall \mathbf{x}} \frac{\mathbf{x}^T \mathbf{A}_s \mathbf{x}}{\mathbf{x}^T \mathbf{x}} \quad (29)$$

with

$$\mathbf{x} = \gamma^{1/2} \hat{\mathbf{q}}_{(i)}, \quad (30)$$

$$\gamma = \Phi^T \mathbf{K} \Phi \quad (31)$$

and

$$\mathbf{A}_s = \gamma^{-1/2} (\Phi^T \mathbf{K}_s \Phi) \gamma^{-1/2}. \quad (32)$$

Since \mathbf{A}_s is symmetric, Π_s^m corresponds to its maximum eigenvalue, according to the Courant–Fischer Minimax theorem [14]. $\mathbf{A}_s \in \mathbb{R}^{n_s \times n_s}$ and is easy to compute since the product $(\Phi^T \mathbf{K}_s \Phi)$ is evaluated only for the degrees of freedom related to the substructure s .

2.5. Optimal sensor placement

It has been shown that the quality of the expansion process is highly dependent on the choice of the measured degrees of freedom. If the modal MECE expansion is used, the best sensor configuration will be the one that optimises the estimation of the modal displacements vector \mathbf{q} of Eq. (14) in some sense. Ref. [15] presents a technique that optimises the set-up for the basic modal projection expansion. It is assumed that the measured vector can be decomposed in two parts:

$$\bar{\mathbf{v}} = \Phi \mathbf{q}^* + \mathbf{n}. \quad (33)$$

The degree of validity of this assumption depends on the richness of the selected modes to generate the subspace where $\bar{\mathbf{v}}$ belongs to. Let us assume that noise \mathbf{n} on the measurements follows:

$$E(\mathbf{nn}^T) = \Psi_0^2 = \varphi_0^2 \mathbf{I},$$

$$E(\mathbf{n}) = \mathbf{0},$$

where E is the expectation operator. The criterion to choice sensors will be given by the minimisation of the covariance matrix for the estimates of the modal displacements for a SEREP expansion:

$$\min \| [E((\mathbf{q} - \mathbf{q}^*)(\mathbf{q} - \mathbf{q}^*)^T)] \|,$$

which can be written (using Eq. (45)) as

$$\min \| \varphi_0^2 [\Phi^T \Phi]^{-1} \|$$

or equivalently

$$\max \| [\Phi^T \Phi] \|.$$

This gives a criterion to select those DOFs that will be erased from the measured set: “The DOFs which do not contribute (or very little) to the norm of $\| \Phi^T \Phi \|$ are useless to be measured”. For convenience, the trace will be used as matrix norm

$$\| \Phi^T \Phi \| = \text{tr}(\Phi^T \Phi)$$

or, exploiting the invariance of the trace:

$$\| \Phi^T \Phi \| = \text{tr}(\Lambda),$$

where Λ is derived from the associated eigenvalue problem

$$(\Phi^T \Phi) \Psi = \Lambda \Psi.$$

Then, the **Efi** vector is defined by

$$\mathbf{Efi} = (\Phi \Psi)^{-2} \Lambda^{-1} \mathbf{i},$$

where -2 indicates a term by term product, and \mathbf{i} is a vector full of unit values. **Efi** outputs the best configuration for a SEREP expansion. Given relation (14), the same can be said for the MECE expansion (11). **Efi** is the optimal set-up for error localisation, when using the MECE error localisation indicator.

According to the steps previously described, Fig. 1 describes the general procedure to define an adequate experimental set-up that assures a given level of quality in the expansion/error localisation.

3. Example

Let us consider the structure displayed in Fig. 2, which represents a rectangular plate with free-free boundary conditions. A summary of the FE model properties is given in Table 1.

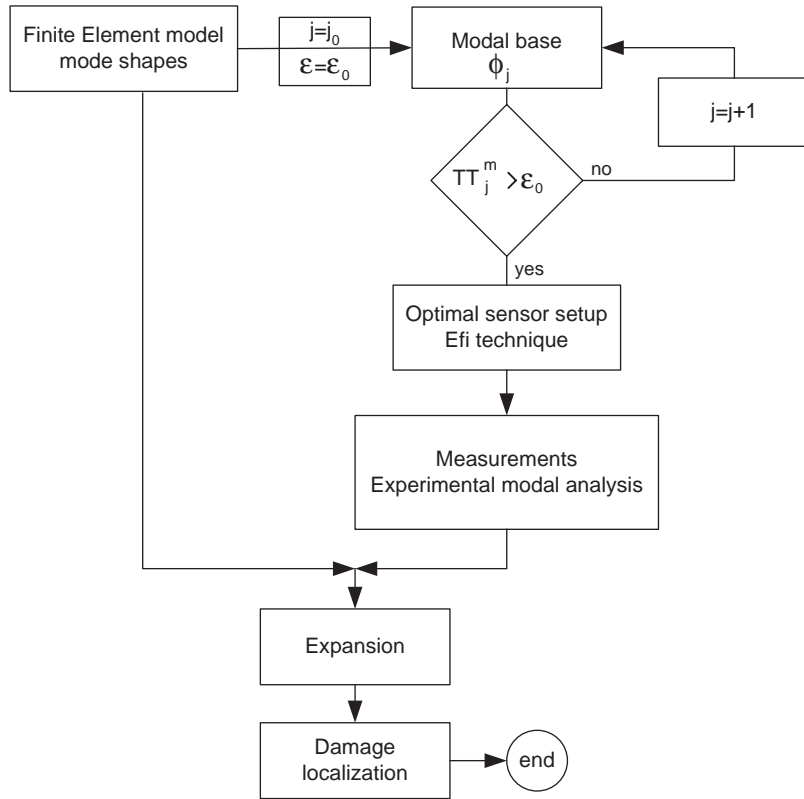


Fig. 1. Damage assessment process.

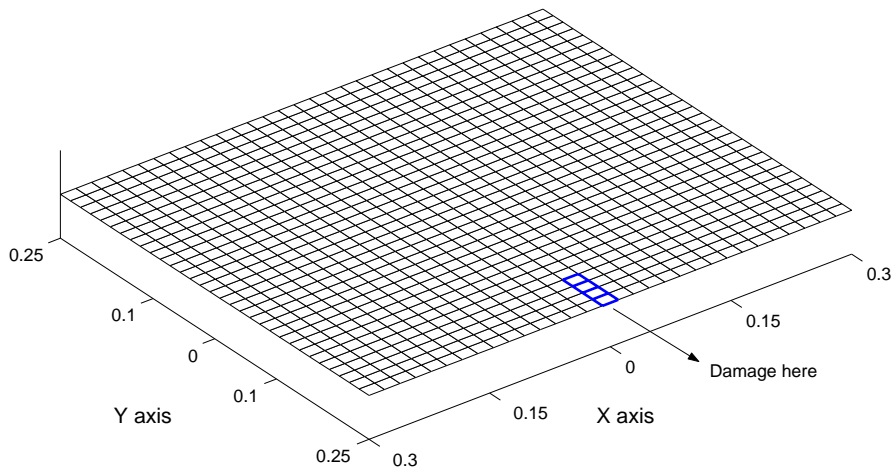


Fig. 2. Structure and perturbed elements.

Table 1
Data properties for the FE model

Properties	Parameters	Value	Unit
General	Young	2.1×10^{11}	N/m ²
	Poisson	0.3	
	Density	7800	kg/m ³
Plates	Elements	31×31	
	Thickness	0.001	m
	Sides length	0.6×0.5	m \times m
	DOFs	3072	
	Nodes	1024	

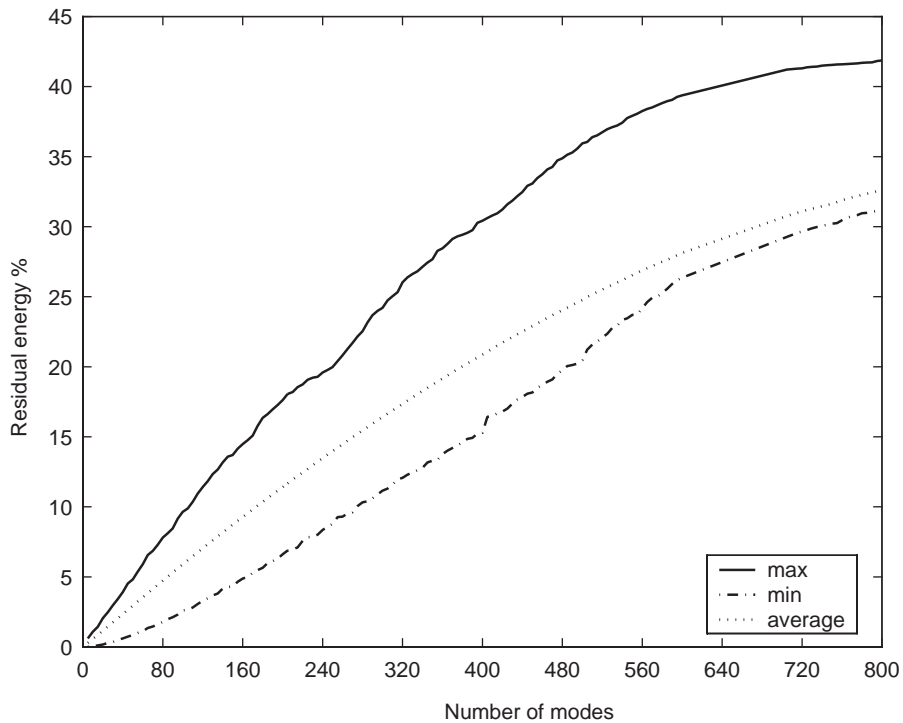


Fig. 3. Π^m vs. the number of eigenmodes.

The purpose of the test is to simulate the experimental measurements of a damaged state of the structure shown in Fig. 2 in order to allow us to build the expanded mode shapes. The influence of the number of modes shapes in the expansion basis and the number of experimental DOFs are analysed to assess a good expansion. After the decisions on the number of modes shapes in the expansion basis and number of experimental measurements are made, the localisation of the damaged elements may be performed. The damage is modelled as a reduction of stiffness in the four elements highlighted in Fig. 2. The reduction is 60% of the elementary stiffness matrix.

3.1. Deciding the number of measured DOFs and the size of the expansion basis

As it was explained in Section 2.3, the residual vector $\mathbf{v} - \mathbf{u}$ will be a linear combination of n_n analytical mode shapes. Therefore, its content of strain energy distribution will give different values for damage detection depending on what the n_n numerical mode shapes are capable to reproduce. To ensure a good level of the residual energy which an element may carry, a minimum number of experimental DOFs must be measured and a minimum number of mode shapes must be in the expansion basis. Fig. 3 shows the evolution of the Π^m indicator as the number of eigenmodes in the expansion basis increases. A large number of modes will produce a higher value for the residual strain energy that an element may concentrate.

The Π^m analysis is performed with an increasing number of eigenmodes, ordered according to their natural frequencies. An alternative approach could be an optimal subset selection, leaving only the numerical eigenmodes which allow a good representation of the experimental behaviour. Fig. 3 shows that considering the first 400 modes in the expansion allows a good localisation, since the Π^m shows peaks up to 30% of the total residual strain energy. The convergence of the Π^m analysis is related to the form of the structure and also to the type and size of elements used in the FE model. In this particular case, the asymptotic behaviour is reached because the experimental structure is very simple and all the elements are equal and have the same size, except for those at the edges of the plate. It is impossible have a 100% for the residual energy stored in an element for the reasons explained in Section 2.3.2.

In general, it is difficult to have an asymptotic behaviour for a structure with a complicated configuration and modelled numerically with elements of different types and sizes.

3.2. Experimental DOFs

3.3. Results

The first three expanded experimental mode shapes used in the localisation are shown in Fig. 7. For the case of the simulated accelerometer mesh, Fig. 4(a), the expansion is done with 40 mode in the expansion basis, since it has only 64 measurements points. The case of Fig. 4(b) is expanded

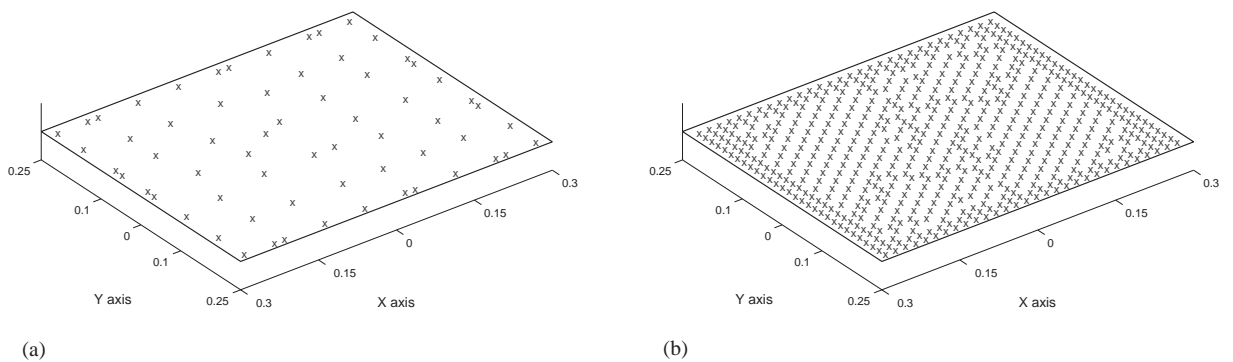


Fig. 4. Sensor set-up for Efl technique: (a) 64 DOFs, (b) 600 DOFs.

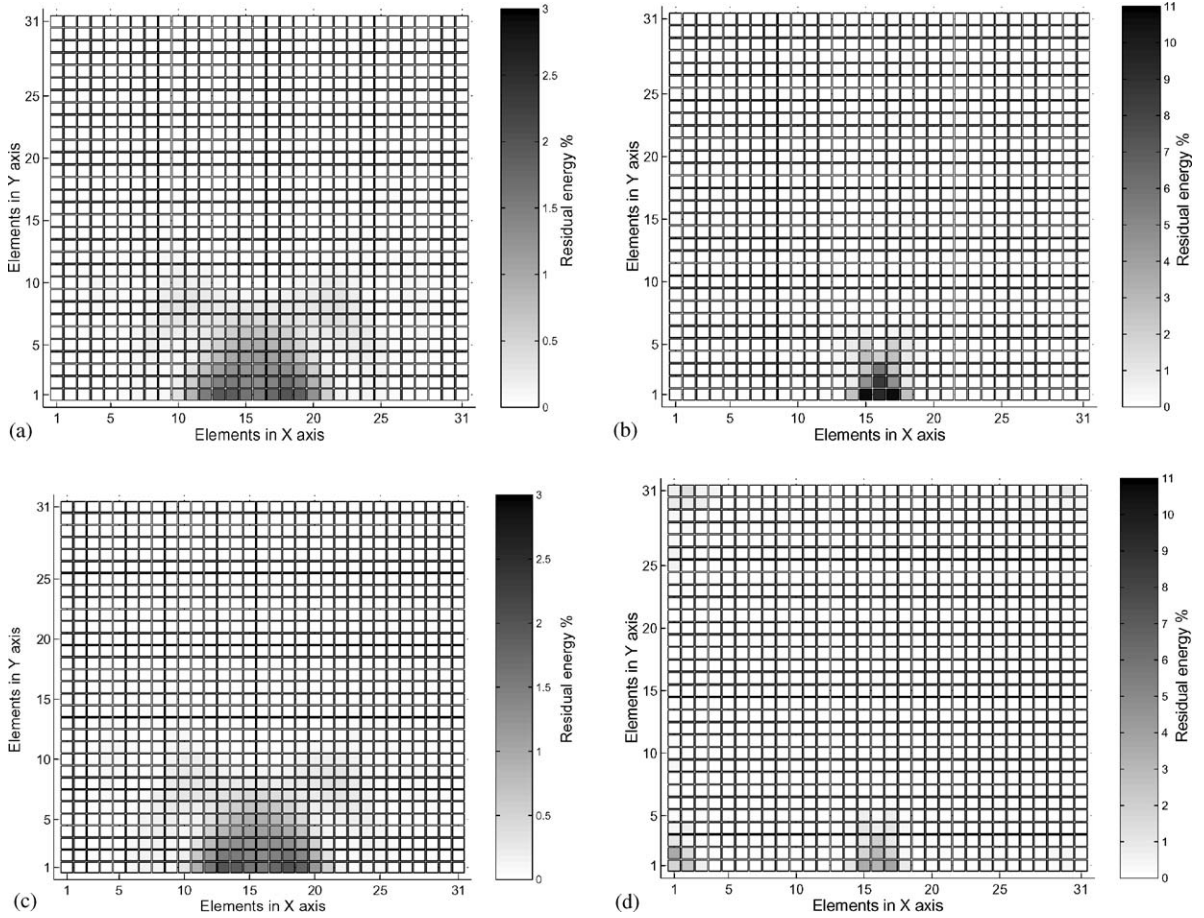


Fig. 5. MECE localisation. Simulated experimental mode #1: (a) 64 DOFs. Noise-free; (b) 600 DOFs. Noise-free; (c) 64 DOFs. 2% noise; (d) 600 DOFs. 2% noise.

with 400 modes in the expansion basis. The reason between the number of eigenvectors in the expansion basis and the number of experimental DOFs is $\frac{2}{3}$ for the two cases. As expected a better localisation is reached with a large number of measurements points and mode shapes in the expansion.

The importance of the number of analytical eigenmodes in the expansion was clearly shown with the Π^m analysis. This indicator is a powerful tool to estimate a priori the localisation limitations associated with the modal base selection. The localisation using a limited expansion basis and less measurements point produces more scattering of the residual energy over the structure. This situation is clearly shown with the black zones in Figs. 5 and 6. A little number of measurements make no difference in the level of residual energy stored in an element. Thus, their quantity is a very important matter. On the other hand a great number of DOFs allow higher levels of elementary residual energy, see residual energy levels reached considering 600 experimental DOFs (Figs. 5(b) and 6(b)). Figs. 5(c), 5(d), 6(c) and 6(d), respectively show the

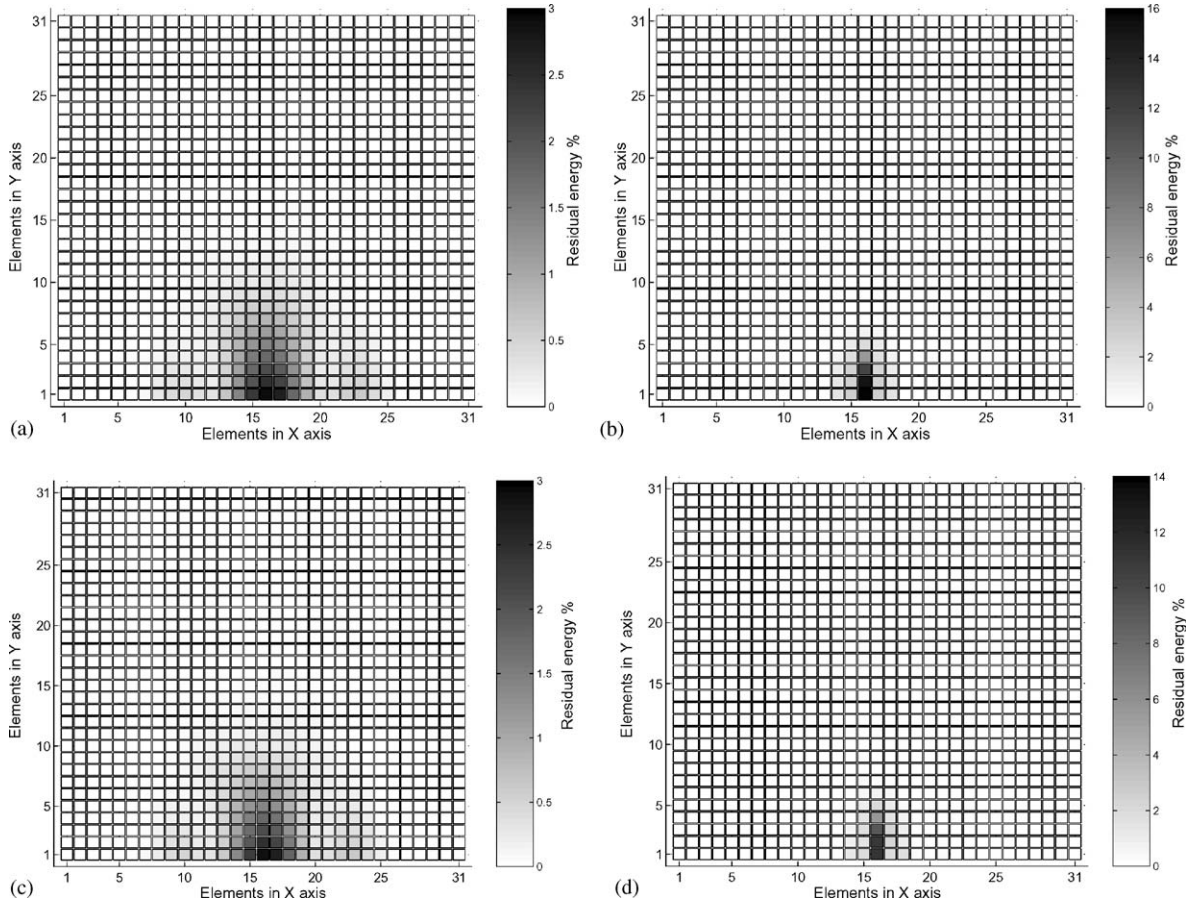


Fig. 6. MECE localisation. Simulated experimental mode #2: (a) 64 DOFs. Noise-free; (b) 600 DOFs. Noise-free; (c) 64 DOFs. 2% noise; (d) 600 DOFs. 2% noise.

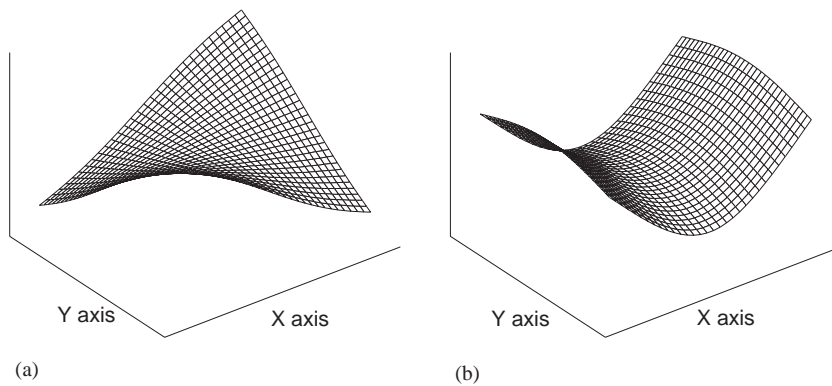


Fig. 7. Simulated experimental modes (11.2 and 14.6 Hz, respectively): (a) First mode; (b) second mode.

Table 2
Maximum residual energy on a perturbed elements

Mode no.	Noise-free		2% noise		
	ω (Hz)	64 DOFs	600 DOFs	64 DOFs	600 DOFs
1	11.2	2.0	10.3	2.0	3.8
2	14.6	2.8	15.5	2.8	14.5

localisation results when the measurements are polluted with a random noise with mean zero and standard deviation 2% of the displacement amplitudes. This level of noise is considered realistic for LDV measurements. Given that the model errors are located on a nodal line of mode #1 (Fig. 7), results are quite sensitive to the existence of noise in the measurements (as described by Eq. (19)). This is not the case for mode #2 where results are much less insensitive (see also Table 2).

4. Conclusions

In this paper a procedure to the expansion/damage assessment process using novel concepts is presented. The current methodology is unique among other approaches since it deals with: (1) size of the expansion basis; (2) number of experimental DOFs; and (3) sensor placement.

A numerical example using a rectangular plate-like structure is used to show the following:

- (1) The damage assessment process is quite sensitive to the number of modes shapes in the expansion basis. In order to verify that the expansion basis is rich enough, we introduced the Π^m indicator which gives the upper bound for the residual energy which may be carried out by a given substructure using modal projection. With this indicator the number of mode shapes in the expansion basis is addressed to guarantee a minimum percentage of total residual energy stored in an element.
- (2) Having a great number of experimental DOFs allow us to consider a great number of numerical eigenmodes in the expansion basis. A consequence of this fact is that the residual force is reproduced in a more accurate way, spreading less residual energy over the structure and detecting only the perturbed elements. Another advantage is that the expansion procedure is reduced since the number of analytical and experimental DOFs became closer.
- (3) A deficient expansion generates a smoothed expanded vector causing a residual energy scattered all over the structure. The sources of these inconveniences are the poorly chosen sensor set-up, the limited number of experimental DOFs and the size of the expansion basis. The example compares two situations, overcoming the problems previously explained, by a sensor placement method, high-spatial density measurements and an indicator for the size of the expansion basis.
- (4) The combined use of the Π^m and the sensor placement method technique provides a good expansion and therefore a suitable damage localisation.

Acknowledgements

The authors wish to acknowledge the partial financial support of this study by the FONdo Nacional de DEsarrollo Científico Y Tecnológico (FONDECYT) of the Chilean government (project 1020810).

References

- [1] R. Pascual, Model based structural damage assessment using vibration measurements. Ph.D. Thesis, (Université de Liege), Belgium, 1999.
- [2] O.S. Salawu, Detection of structural damage through changes in frequency: a review, *Engineering Structures* 19 (9) (1997) 718–723.
- [3] C.P. Ratcliffe, Damage detection using a modified Laplacian operator on mode shape data, *Journal of Sound and Vibration* 204 (3) (1997) 505–517.
- [4] K. Pandey, M. Biswas, M.M. Samman, Damage detection from changes in curvature mode shapes, *Journal of Sound and Vibration* 145 (1991) 321–332.
- [5] Z.Y. Shi, S.S. Law, L.M. Zhang, Structural damage localisation from modal strain energy change, *Journal of Sound and Vibration* 218 (5) (1998) 825–844.
- [6] U. Lee, J. Shin, A frequency-domain method of structural damage identification formulated from the dynamic stiffness equation of motion, *Journal of Sound and Vibration* 257 (4) (2002) 615–634.
- [7] W.X. Ren, D.J. Yu, J.Y. Shen, Structural damage identification using residual modal forces, *Proceedings of XXI International Modal Analysis Conference*, Florida, 2003.
- [8] A. Messina, E.J. Williams, T. Contursi, Structural damage detection by a sensitivity and statistical based method, *Journal of Sound and Vibration* 216 (5) (1998) 791–808.
- [9] J.T. Kim, N. Stubbs, Improved damage identification method based on modal information, *Journal of Sound and Vibration* 252 (2) (2002) 223–238.
- [10] W. Gawronski, J.T. Sawicki, Structural damage detection using modal norms, *Journal of Sound and Vibration* 229 (1) (2000) 194–198.
- [11] S.K. Thyagarajan, M.J. Schulz, P.F. Pai, J. Chung, Detecting structural damage using frequency response functions, *Journal of Sound and Vibration* 210 (1) (1998) 162–170.
- [12] J. O’Callahan, P. Avitabile, System equivalent reduction expansion process (SEREP), *Proceedings of the 7th International Modal Analysis Conference*, Nevada, 1989, pp. 29–37.
- [13] M. Geradin, D. Rixen, *Theorie Des Vibrations*, Masson, Paris, 1996.
- [14] G.H. Golub, C.F. Van Loan, *Matrix Computations*, John Hopkins University Press, Baltimore, MD, 1996.
- [15] D.C. Kammer, L. Yao, Enhancement of on-orbit modal identification of large space structures through sensor placement, *Journal of Sound and Vibration* 171 (1) (1994) 119–139.